Available online at www.sciencedirect.com
SCIENCE DIRECT®
Journal of Solid State Chemistry 178 (2005) 1247–1253
JOURNAL OF SOLID STATE CHEMISTRY
www.elsevier.com/locate/jssc

On the crystal chemistry of $Tm_2Ni_{1.896(4)}In$, $Tm_{2.22(2)}Ni_{1.81(1)}In_{0.78(2)}$, $Tm_{4.83(3)}Ni_2In_{1.17(3)}$, and Er_5Ni_2In

Mar'yana Lukachuk[a], Yaroslav M. Kalychak[b], Mariya Dzevenko[b], Rainer Pöttgen[a,*]

[a]*Institut für Anorganische und Analytische Chemie and NRW Graduate School of Chemistry, Universität Münster, Corrensstrasse 36, Münster D-48149, Germany*

[b]*Inorganic Chemistry Department, Ivan Franko National University of Lviv, Kyryla and Mephodiya Street 6, Lviv 79005, Ukraine*

Received 26 October 2004; received in revised form 16 November 2004; accepted 22 November 2004

Abstract

The rare earth–nickel-indides $Tm_2Ni_{1.896(4)}In$, $Tm_{2.22(2)}Ni_{1.81(1)}In_{0.78(2)}$, $Tm_{4.83(3)}Ni_2In_{1.17(3)}$, and Er_5Ni_2In were synthesized from the elements by arc-melting and subsequent annealing for the latter three compounds. Three indides were investigated by X-ray powder and single crystal diffraction: Mo_2FeB_2 type, $P4/mbm$, $Z = 2$, $a = 731.08(4)$, $c = 358.80(3)$ pm, $wR_2 = 0.0201$, 178 F^2 values, 13 variables for $Tm_2Ni_{1.896(4)}In$, $a = 734.37(7)$, $c = 358.6(1)$ pm, $wR_2 = 0.0539$, 262 F^2 values, 14 variables for $Tm_{2.22(2)}Ni_{1.81(1)}In_{0.78(2)}$, and Mo_5SiB_2 type, $I4/mcm$, $a = 751.0(2)$, $c = 1317.1(3)$ pm, $wR_2 = 0.0751$, 317 F^2 values, 17 variables for $Tm_{4.83(3)}Ni_2In_{1.17(3)}$. X-ray powder data for Er_5Ni_2In revealed $a = 754.6(2)$ and $c = 1323.3(5)$ pm. The Mo_2FeB_2 type structures of $Tm_2Ni_{1.896(4)}In$ and $Tm_{2.22(2)}Ni_{1.81(1)}In_{0.78(2)}$ are intergrowths of slightly distorted CsCl and AlB_2 related slabs, however, with different crystal chemical features. The nickel sites within the AlB_2 slabs are not fully occupied in both indides. Additionally In/Tm mixing is possible at the center of the CsCl slab, as is evident from the structure refinement of $Tm_{2.22(2)}Ni_{1.81(1)}In_{0.78(2)}$. The Mo_5SiB_2 type structures of $Tm_{4.83(3)}Ni_2In_{1.17(3)}$ and Er_5Ni_2In can be considered as an intergrowth of distorted $CuAl_2$ and U_3Si_2 related slabs in an $ABA'B'$ stacking sequence along the c-axis. Again, one thulium site shows Tm/In mixing. The U_3Si_2 related slab has great structural similarities with the Mo_2FeB_2 type structure of $Tm_2Ni_{1.896(4)}In$ and $Tm_{2.22(2)}Ni_{1.81(1)}In_{0.78(2)}$. The crystal chemical peculiarities and chemical bonding in these intermetallics are briefly discussed.

Keywords: Intermetallic compounds; Crystal structure; Indium

1. Introduction

Phase analytical investigations in the *RE*–Ni–In systems (*RE* = rare earth metal) revealed the existence of more than 180 ternary $RE_xNi_yIn_z$ indides [1–4, and Ref. therein], Several isothermal sections of the *RE*–Ni–In phase diagrams have already been constructed. Although most of the ternary phases are known with respect to their approximate compositions (determined via metallography, EDX, and X-ray powder data), for several phases the crystal structures are still unknown. In many cases the structures of the unknown phases are complex or they exhibit homogeneity ranges. Only precise single crystal data can help for the structure determination and thus, suitable crystal growth experiments are important.

The Tm–Ni–In system was so far characterized by the intermetallic compounds $TmNi_4In$ [5], $Tm_{10}Ni_9In_{20}$ [6], TmNiIn [7,8], $Tm_5Ni_2In_4$ [9], Tm_2Ni_2In, and $Tm_2Ni_{2-x}In$ [10,11]. Recent phase analytical reinvestigations in this system revealed the new thulium-rich compound $Tm_{14-x}Ni_{3+y}In_{3+x-y}$ [12]. Single crystal studies of various samples around the equiatomic composition showed a substantial homogeneity range

*Corresponding author. Fax: +49 251 83 36002.
E-mail addresses: kalychak@franko.lviv.ua (Y.M. Kalychak), pottgen@uni-muenster.de (R. Pöttgen).

0022-4596/$ - see front matter © 2004 Elsevier Inc. All rights reserved.
doi:10.1016/j.jssc.2004.11.023

$TmNi_{1-x-y}In_{1+x}$ [13]. The indides Tm_2Ni_2In, and $Tm_2Ni_{1.78}In$ [10,11] have only been investigated on the basis of X-ray powder data. Stoichiometric Tm_2Ni_2In adopts the orthorhombic Mn_2AlB_2 structure, space group *Cmmm*, while $Tm_2Ni_{2-x}In$ with small defects on the nickel site adopts the tetragonal Mo_2FeB_2 type, space group *P*4/*mbm*. With special annealing procedures it was now possible to grow small single crystals (up to 100 μm) of compounds with compositions close to $Tm_2Ni_{2-x}In$ ($x \approx 0.22$, this is approximately the limit of the homogeneity range). These studies confirmed the nickel defects, but additionally we also found Tm/In mixing for $Tm_{2.22(2)}Ni_{1.81(1)}In_{0.78(2)}$. Samples with a higher rare earth metal content revealed the new indides $Tm_{4.83(3)}Ni_2In_{1.17(3)}$ and Er_5Ni_2In with Mo_5SiB_2 type structure. The synthesis, structure determination and crystal chemistry of these phases are reported herein. A preliminary account of some of this work was given recently at a conference [12].

2. Experimental

2.1. Synthesis

Starting materials for the preparation of $Tm_2Ni_{1.896(4)}In$, $Tm_{2.22(2)}Ni_{1.81(1)}In_{0.78(2)}$, $Tm_{4.83(3)}Ni_2In_{1.17(3)}$, and Er_5Ni_2In were ingots of erbium and thulium (Johnson-Matthey), nickel wire (∅ 0.38 mm, Johnson-Matthey), and indium tear drops (Johnson-Matthey), all with stated purities better than 99.9%. All samples were prepared directly from the elements via arc-melting [14] under an atmosphere of ca. 600 mbar argon. The argon was purified before over titanium sponge (900 K), silica gel, and molecular sieves. All samples were turned over and remelted two times in the arc-melting crucible in order to achieve homogeneity. The weight losses were always smaller than 0.5 wt%.

The $Tm_2Ni_{1.896(4)}In$ crystals were obtained from a sample of the starting composition 2 Tm:1.8 Ni:1 In. The sample was already well crystallized after the arc-melting procedure. No further annealing was necessary. Single crystals of the thulium-richer phase $Tm_{2.22(2)}Ni_{1.81(1)}In_{0.78(2)}$ were obtained from a sample with the atomic ratio 11 Tm:6 Ni:3 In. For crystal growth, the arc-melted button was sealed in a small tantalum tube, which was sealed in a silica ampoule for oxidation protection. First the sample was heated for 3 h in a box furnace at 1320 K, followed by slow cooling to 1070 K at a rate of 5 K/h and then to 770 K at a rate of 15 K/h. Finally, the sample was quenched by radiative heat loss inside the furnace.

$Tm_{4.83(3)}Ni_2In_{1.17(3)}$ originated from a sample prepared by arc-melting of the elements in the 62:27:11 atomic ratio. In order to obtain single crystals, pieces of the arc-melted product were sealed in a tantalum tube, which was then enclosed in an evacuated silica tube. The tube was first heated at 1250 K for 3 h and then cooled to room temperature at a rate of 5 K/h. Small single crystals could be separated from this sample after mechanical fragmentation. Two other pieces of the sample were sealed in evacuated quartz ampoules and annealed in a box furnace. The first one at 670 K for one month and the second one at 1170 K for one week.

Er_5Ni_2In was prepared from a 5:2:1 sample by arc-melting. One piece of the sample was homogenized by annealing in an evacuated quartz ampoule at 1170 K during one week. After the annealing procedure, the sample was quenched in cold water. No single crystals were available either after the melting procedure or after slow cooling of the sample in a box furnace.

The brittle samples were all stable in air as compact pieces as well as fine-grained powders. Single crystals exhibit metallic luster.

2.2. X-ray powder diffraction

The samples were characterized through Guinier powder patterns (imaging plate technique, Fujifilm BAS-1800) with Cu$K\alpha_1$ radiation and α-quartz ($a = 491.30$, $c = 540.46$ pm) as an internal standard. The lattice parameters (Table 1) were obtained from least-squares fits of the Guinier data. The correct indexing was ensured through intensity calculations [15] using the positional parameters of the structure refinements. With the exception of $Tm_{2.22}Ni_{1.81}In_{0.78}$, the lattice parameters of the powders and the single crystals agreed well (Table 1). The small discrepancy is most likely due to the homogeneity range.

2.3. Scanning electron microscopy

The crystals investigated on the diffractometer have been analyzed in a scanning electron microscope (LEICA 420i) through energy dispersive analyses of X-rays. TmF_3, nickel metal, and InAs were used as standards. No impurity elements heavier than sodium have been observed. The experimentally determined compositions of 41 ± 2 at% Tm:36 ± 2 at% Ni:23 ± 2 at% In for $Tm_2Ni_{1.896}In$ (41:39:20), 45 ± 3 at% Tm:34 ± 3 at% Ni:21 ± 3 at% In for $Tm_{2.22}Ni_{1.81}In_{0.78}$ (46:38:16), and 62 ± 2 at% Tm:24 ± 2 at% Ni:14 ± 2 at% In for $Tm_{4.83}Ni_2In_{1.17}$ (60:25:15) were close to the compositions calculated from the structure refinements (in parentheses). The uncertainties of the measurements of ±2–3 at% arise from the irregular surface of the single crystals.

2.4. Structure refinements

Irregularly shaped single crystals of the thulium containing phases were selected from the crushed

Table 1
Lattice parameters of tetragonal Mo_2FeB_2 or Mo_5SiB_2 type compounds

Compound	Str. Type	a (pm)	c (pm)	V (nm^3)
$Tm_2Ni_{1.78}In$ [11]	Mo_2FeB_2	729.3(4)	364.4(4)	0.1938
$Tm_2Ni_{1.896(4)}In$[a]	Mo_2FeB_2	731.08(4)	358.80(3)	0.1918
$Tm_2Ni_{1.896(4)}In$[b]	Mo_2FeB_2	730.65(7)	358.6(1)	0.1914
$Tm_{2.22(2)}Ni_{1.81(1)}In_{0.78(2)}$[a]	Mo_2FeB_2	737.5(1)	360.2(1)	0.1959
$Tm_{2.22(2)}Ni_{1.81(1)}In_{0.78(2)}$[b]	Mo_2FeB_2	734.37(7)	358.6(1)	0.1934
$Tm_{4.83(3)}Ni_2In_{1.17(3)}$[a]	Mo_5SiB_2	751.0(2)	1317.1(3)	0.7430
$Tm_{4.83(3)}Ni_2In_{1.17(3)}$[b]	Mo_5SiB_2	752.16(7)	1315.9(1)	0.7445
Er_5Ni_2In[a]	Mo_5SiB_2	754.6(2)	1323.3(5)	0.7535

[a]Lattice parameters from Guinier powder data.
[b]Lattice parameters from diffractometer measurements.

samples and first examined on Buerger precession cameras (white Mo radiation, Fujifilm BAS-1800 imaging plate system) in order to check the quality for intensity data collection. The data sets for the three crystals were collected at room temperature by use of a four-circle diffractometer (CAD4) with graphite monochromatized Mo$K\alpha$ radiation (71.073 pm) and a scintillation counter with pulse height discrimination. The scans were performed in the $\omega/2\theta$ mode. Empirical absorption corrections were applied on the basis of Ψ-scan data followed by spherical absorption corrections. All relevant crystallographic data and details for the data collections are summarized in Table 2.

The isotypism of the $Tm_2Ni_{1.896(4)}In$ and $Tm_{2.22(2)}Ni_{1.81(1)}In_{0.78(2)}$ crystals with the tetragonal Mo_2FeB_2 type was already evident from the Guinier powder data. Analyses of the diffractometer data sets were compatible with space group $P4/mbm$. The atomic parameters of Ce_2Pt_2In [16] were taken as starting values and both structures were refined with SHELXL-97 (full-matrix least-squares on F^2) [17] with anisotropic displacement parameters for all atoms. Both crystals revealed a large equivalent isotropic displacement parameter for the $4g$ nickel site, indicating a smaller scattering power. Refinement of the occupancy parameters showed nickel occupancies of only 94.8(4)% and 90.7(9)%. For the second crystal, the equivalent isotropic displacement parameter of the indium site was too small. In agreement with our recent results on the solid solution $Tm_{14-x}Ni_{3+y}In_{3+x-y}$ [12] and the EDX results, we refined this position with a mixed Tm/In occupancy, leading to the refined compositions $Tm_2Ni_{1.896(4)}In$ and $Tm_{2.22(2)}Ni_{1.81(1)}In_{0.78(2)}$ for the crystals investigated.

Analyses of the third data set revealed high tetragonal Laue symmetry $4/mmm$, a body-centered lattice and additionally the extinction condition $0kl$ only observed for l, $(k) = 2n$. This led to the possible space groups $I4cm$, $I\bar{4}c2$ and $I4/mcm$ of which the centrosymmetric group was found to be correct during the structure refinement. The starting atomic parameters were deduced from an automatic interpretation of direct methods with SHELXS-97 [18] and the structure was refined with anisotropic displacement parameters for all atoms. Similar to $Tm_{2.22(2)}Ni_{1.81(1)}In_{0.78(2)}$, also the Tm1 site showed a mixed Tm/In occupancy, leading to the refined composition $Tm_{4.83(3)}Ni_2In_{1.17(3)}$ for the crystal investigated, in good agreement with the EDX analysis. The final difference Fourier syntheses were flat for all three data sets (Table 2). The positional parameters and interatomic distances of the refinements are listed in Tables 3 and 4. Further data on the structure refinements are available.[1]

3. Discussion

The indides $Tm_2Ni_{1.896}In$ and $Tm_{2.22}Ni_{1.81}In_{0.78}$ (Fig. 1) crystallize with the tetragonal Mo_2FeB_2 type structure [19], a ternary ordered version of the U_3Si_2 type [20,21]. Since the crystal chemistry of intermetallics within the U_3Si_2 family has recently been reviewed in detail [22], here we only focus on the main crystal chemical peculiarities. $Tm_2Ni_{2-x}In$ with $x \approx 0.22$ has already been reported on the basis of phase analytical investigations and X-ray powder diffraction [10,11]. The present single crystal study fully confirms these findings. It is worthwhile to note, that the tetragonal Mo_2FeB_2 type is only formed, when the nickel sites have a considerable degree of defects. With a full nickel occupancy the structure switches to the orthorhombic Mn_2AlB_2 type [23].

Furthermore we observed another structural feature for this family of indides. The second crystal which originated from a thulium-richer sample showed In/Tm mixing on the $2a$ site, the center of the square prisms (Fig. 1). So far, such a substitution has only been observed for the solid solution $U_{2+x}Co_2Ga_{1-x}$ [24] and

[1]Details may be obtained from: Fachinformationszentrum Karlsruhe, D-76344 Eggenstein-Leopoldshafen (Germany), by quoting the Registry No's. CSD–414499 ($Tm_2Ni_{1.896}In$), CSD–414498 ($Tm_{2.22}Ni_{1.81}In_{0.78}$), and CSD–414497 ($Tm_{4.83}Ni_2In_{1.17}$).

Table 2
Crystal data and structure refinements for $Tm_2Ni_{1.896(4)}In$, $Tm_{2.22(2)}Ni_{1.81(1)}In_{0.78(2)}$, and $Tm_{4.83(3)}Ni_2In_{1.17(3)}$

Empirical formula	$Tm_2Ni_{1.896(4)}In$	$Tm_{2.22(2)}Ni_{1.81(1)}In_{0.78(2)}$	$Tm_{4.83(3)}Ni_2In_{1.17(3)}$
Molar mass	563.94 g/mol	571.14 g/mol	1067.15 g/mol
Space group, Z	*P4/mbm*, 2	P4/*mbm*, 2	*I4/mcm*, 4
Unit cell dimensions	see Table 1	see Table 1	see Table 1
Calculated density	9.77 g/cm^3	9.81 g/cm^3	9.54 g/cm^3
Crystal size	$20\times20\times60\,\mu m^3$	$10\times20\times60\,\mu m^3$	$20\times20\times60\,\mu m^3$
Transm. ratio (max/min)	2.63	2.36	2.08
Absorption coefficient	60.6 mm^{-1}	63.4 mm^{-1}	65.3 mm^{-1}
$F(000)$	480	484	1786
θ range	4° to 30°	4° to 35°	3° to 30°
Range in *hkl*	±10, ±10, ±5	±11, ±11, ±5	±10, ±10, +18
Total no. reflections	2066	3172	2189
Independent reflections	178 ($R_{int}=0.0566$)	262 ($R_{int}=0.0830$)	317 ($R_{int}=0.1378$)
Reflections with $I>2\sigma(I)$	165 ($R_{sigma}=0.0192$)	241 ($R_{sigma}=0.0268$)	206 ($R_{sigma}=0.0621$)
Data/parameters	178/13	262/14	317/17
Goodness-of-fit on F^2	1.145	1.465	1.109
Final R indices [$I>2\sigma(I)$]	$R_1=0.0122$	$R_1=0.0308$	$R_1=0.0274$
	$wR_2=0.0198$	$wR_2=0.0529$	$wR_2=0.0581$
R indices (all data)	$R_1=0.0152$	$R_1=0.0361$	$R_1=0.0710$
	$wR_2=0.0201$	$wR_2=0.0539$	$wR_2=0.0751$
Extinction coefficient	0.0022(3)	0.0054(6)	0.00035(7)
Largest diff. peak and hole	0.95/−1.28 e/Å^3	2.05/−2.67 e/Å^3	2.97/−3.29 e/Å^3

Table 3
Atomic coordinates and isotropic displacement parameters (pm^2) for $Tm_2Ni_{1.896(4)}In$, $Tm_{2.22(2)}Ni_{1.81(1)}In_{0.78(2)}$ and $Tm_{4.83(3)}Ni_2In_{1.17(3)}$

Atom	Wyckoff position	Occupancy %	x	y	z	U_{eq}
$Tm_2Ni_{1.896(4)}In$ (space group P4/mbm)						
Tm	4*h*	100	0.17447(3)	$x+1/2$	1/2	75(1)
Ni	4*g*	94.8(4)	0.37916(10)	$x+1/2$	0	96(4)
In	2*a*	100	0	0	0	81(2)
$Tm_{2.22(2)}Ni_{1.81(1)}In_{0.78(2)}$ (space group P4/mbm)						
Tm1	4*h*	100	0.17057(6)	$x+1/2$	1/2	115(2)
Ni	4*g*	90.7(9)	0.3768(2)	$x+1/2$	0	110(6)
In/Tm2	2*a*	78(2)/22(2)	0	0	0	109(4)
$Tm_{4.83(3)}Ni_2In_{1.17(3)}$ (space group I4/mcm)						
Tm1/In2	4*c*	83(3)/17(3)	0	0	0	115(6)
Tm2	16*l*	100	0.15842(7)	$x+1/2$	0.13671(7)	131(3)
Ni	8*h*	100	0.6297(3)	$x+1/2$	0	119(7)
In1	4*a*	100	0	0	1/4	125(6)

U_{eq} is defined as one-third of the trace of the orthogonalized U_{ij} tensor.

for $U_{2.1}Fe_2Sn_{0.9}$ [25]. In the *RE–T–X* systems only mixed positions containing transition metals and *p*-elements have been observed [26,27].

A projection of the $Tm_2Ni_{1.896}In$ structure onto the *xy* plane is presented in Fig. 1. From a geometrical point of view, the structure consists of two different layers: the nickel and indium atoms build a [$Ni_{1.896}In$] network at $z=0$ and all thulium atoms are located between these networks at $z=1/2$. The thulium atoms form square prisms around the indium atoms and distorted trigonal prisms around the nickel atoms. Hence, the $Tm_2Ni_{1.896}In$ structure can be considered as an intergrowth of distorted AlB_2 and CsCl related slabs of compositions $TmNi_{2-x}$ and TmIn. While TmIn [28] with CsCl type structure exists, $TmNi_2$ [29,30] adopts the structure of the cubic Laves phase $MgCu_2$. The Tm–In distance of 324 pm in $Tm_2Ni_{1.896}In$ corresponds to that one in binary TmIn and is significantly shorter than the sum of the atomic radii of thulium and indium (338 pm) [31].

The Tm–Ni distances of 277 and 283 pm within the distorted AlB_2 slabs are significantly shorter than those in the [$TmNi_{12}$] icosahedron of $TmNi_2$ (295 pm) [30] with $MgCu_2$ type structure. Thus, a considerable

Table 4
Interatomic distances (pm), calculated with the lattice parameters taken from X-ray single crystal data of $Tm_{2.22(2)}Ni_{1.81(1)}In_{0.78(2)}$

$Tm_2Ni_{1.896(4)}In$											
Tm:	2	Ni	277.4(1)	Ni:	1	Ni	249.9(2)	In:	4	Ni	290.9(1)
	4	Ni	283.4(1)		2	Tm	277.4(1)		8	Tm	324.2(1)
	4	In	324.2(1)		4	Tm	283.4(1)		2	In	358.8(1)
	2	Tm	358.8(1)		2	In	290.9(1)				
	1	Tm	360.8(1)								
	4	Tm	381.9(1)								
$Tm_{2.22(2)}Ni_{1.81(1)}In_{0.78(2)}$											
Tm1:	2	Ni	279.3(2)	Ni:	1	Ni	255.9(4)	In/Tm2:	4	Ni	291.1(1)
	4	Ni	282.7(1)		2	Tm1	279.3(2)		8	Tm1	326.1(1)
	4	In/Tm2	326.1(1)		4	Tm1	282.7(1)		2	In/Tm2	358.6(1)
	1	Tm1	354.3(1)		2	In/Tm2	291.1(1)				
	2	Tm1	358.6(1)								
	4	Tm1	385.3(1)								
$Tm_{4.83(3)}Ni_2In_{1.17(3)}$											
Tm1/In2:	4	Ni	294.6(2)	Tm2:	2	Ni	282.3(2)	Ni:	1	Ni	275.6(7)
	2	In1	329.3(1)		1	Ni	288.2(3)		4	Tm2	282.3(2)
	8	Tm2	335.2(1)		2	In	319.7(1)		2	Tm2	288.2(3)
					2	Tm1/In2	335.2(1)		2	Tm1/In2	294.6(2)
					1	Tm2	336.5(2)	In1:	8	Tm2	319.7(1)
					1	Tm2	356.2(2)		2	Tm1/In2	329.3(1)
					1	Tm2	360.1(2)				
					2	Tm2	381.7(2)				
					4	Tm2	399.9(1)				

The distances for $Tm_2Ni_{1.896(4)}In$ and $Tm_{4.83(3)}Ni_2In_{1.17(3)}$ have been calculated with the powder lattice parameters. All distances shorter than 500 pm (Tm–Tm, Tm–In, In–In), 480 pm (Tm–Ni), 460 pm (Ni–In), and 355 pm (Ni–Ni) are listed.

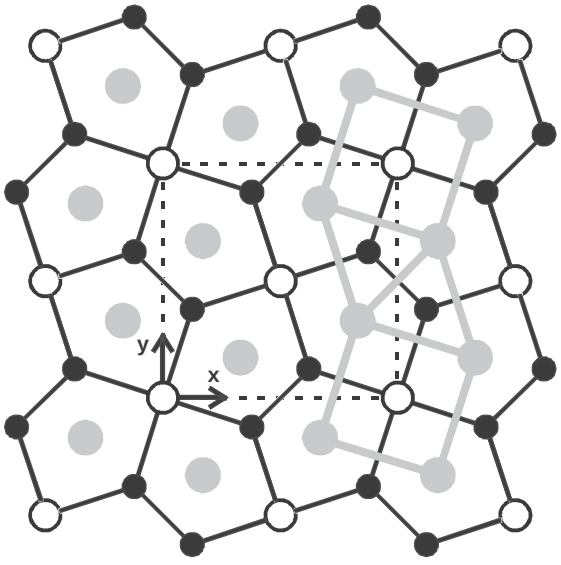

Fig. 1. Projection of the $Tm_2Ni_{1.896(4)}In$ structure onto the *xy* plane. Thulium, nickel, and indium atoms are drawn as grey, black filled, and open circles, respectively. The two-dimensional $[Ni_{1.896}In]$ network at $z = 0$ as well as the trigonal and square prismatic thulium slabs at $z = 1/2$ are emphasized.

degree of Tm–Ni bonding in $Tm_2Ni_{1.896}In$ can be assumed. This agrees with an extended Hückel band structure examination of isotypic Sc_2Ni_2In [32], where the strongest bonding interactions have been observed for the Sc–Ni contacts, followed by Sc–In and Ni–In.

Within the two-dimensional $[Ni_{1.896}In]$ network (Fig. 1), each indium atom has a square planar nickel coordination at Ni–In distances of 291 pm, close to the sum of the atomic radii of 288 pm [31], indicating significant Ni–In interactions. The Ni–Ni distances of 250 pm within the distorted AlB_2 slabs are equal to those in *fcc* nickel (249 pm) [33]. Thus, chemical bonding in $Tm_2Ni_{1.896}In$ is mainly governed by strong Tm–Ni and Tm–In interactions. These distances become longer in $Tm_{2.22}Ni_{1.81}In_{0.78}$, where 22% of the indium atoms in the 2*a* site are substituted by the larger thulium atoms. Another consequence of this substitution is a stronger distortion in the AlB_2 related slabs (Fig. 2). Due to these geometrical constrains (see the Tm–Tm–Tm angle in Fig. 2) the occupancy of the Ni position in $Tm_{2.22}Ni_{1.81}In_{0.78}$ is only 90.7%—a bit lower than in $Tm_2Ni_{1.896}In$, 94.8%.

$Tm_{4.83}Ni_2In_{1.17}$ and Er_5Ni_2In are the first representatives for ternary indides with the tetragonal Mo_5SiB_2 type structure [34], a ternary ordered variant of the Cr_5B_3 type [35]. $Tm_{4.83}Ni_2In_{1.17}$ was investigated on the basis of X-ray powder and single crystal data, while no crystals were available for the sample with the Er_5Ni_2In composition. The latter has been characterized only through its Guinier powder diagram.

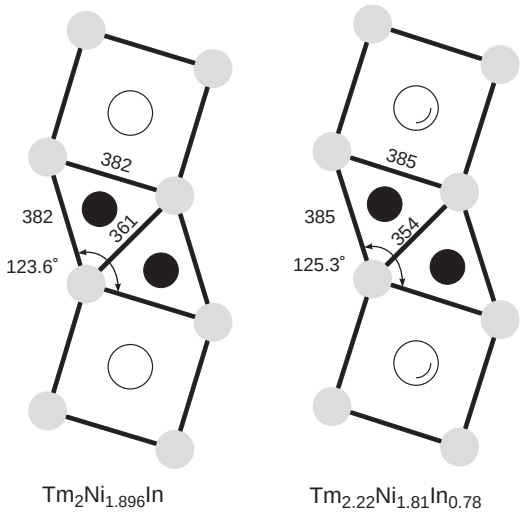

Fig. 2. Cutouts of the $Tm_2Ni_{1.896(4)}In$ and $Tm_{2.22(2)}Ni_{1.81(1)}In_{0.78(2)}$ structures. Thulium, nickel, and indium atoms are drawn as grey, black filled, and open circles, respectively. Atoms marked with a crescent indicate Tm/In mixing. Relevant interatomic distances and bond angles are emphasized.

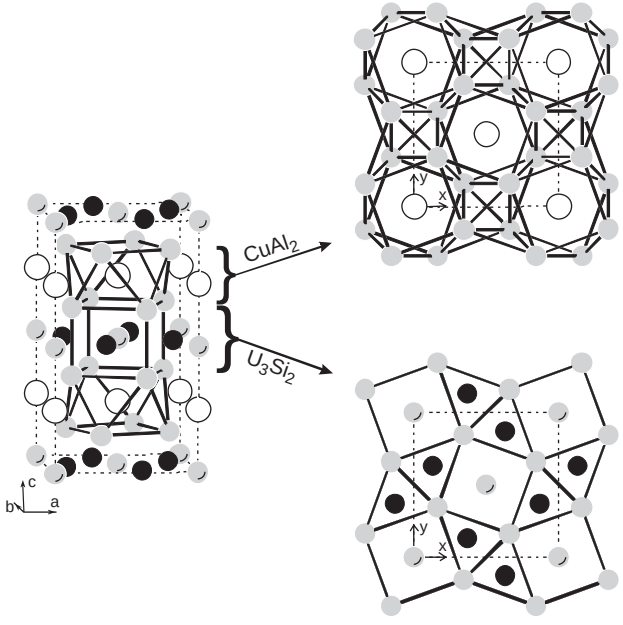

Fig. 3. Crystal structure of $Tm_{4.83(3)}Ni_2In_{1.17(3)}$ viewed approximately along the *b*-axis. Thulium, nickel, and indium atoms are drawn as grey, black filled, and open circles, respectively. Atoms marked with a crescent indicate Tm/In mixing. The chain of alternating square prisms and antiprisms is emphasized. At the right-hand part of the drawing cutouts of the $CuAl_2$ and U_3Si_2 related slabs are shown as projections along the *c*-axis. For details see text.

The $Tm_{4.83}Ni_2In_{1.17}$ structure (Fig. 3) is built up from columns of alternating face-sharing tetragonal prisms and antiprisms formed by the thulium atoms running along the *c* direction. The antiprisms are centered by indium atoms, while the central position in the square prisms is occupied by a mixture of thulium and indium atoms.

From a geometrical point of view the structure can be described as an intergrowth of $CuAl_2$ and U_3Si_2 related slabs of compositions Tm_2In and $(Tm/In)_3Ni_2$. The coloring of the U_3Si_2 related layer is the same as in $Tm_{2.22}Ni_{1.81}In_{0.78}$. Only the Tm/In ratio in the centres of the square thulium prisms is different. The higher occupancy of this position by thulium atoms (83% Tm and 17% In) in $Tm_{4.83}Ni_2In_{1.17}$ results in longer distances within that slab as compared to those in $Tm_{2.22}Ni_{1.81}In_{0.78}$, where the Tm/In ratio is 22:78. The Tm–Ni contacts of 282 and 288 pm, however, still belong to the strongest ones in this structure. The change in the interatomic distances is most pronounced for the AlB_2 related slab. The Ni–Ni distances of 276 pm in $Tm_{4.83}Ni_2In_{1.17}$ are about 20 pm longer than those in the related Mo_2FeB_2 type compounds.

The $CuAl_2$ related slab is composed of $[InTm_8]$ square antiprisms, which are connected via empty thulium tetrahedra. The latter are characterized by very short Tm–Tm distances of 335 pm, which are much shorter than the average Tm–Tm distance of 360 pm in *hcp* thulium [33]. This slab is governed by strong Tm–In interactions with Tm–In distances of 320 pm, which are even shorter than in $Tm_2Ni_{1.896}In$ and significantly shorter than the sum of the atomic radii of thulium and indium (338 pm) [31].

The coordination polyhedra of the $Tm_{4.83}Ni_2In_{1.17}$ structure are shown in Fig. 4. The Tm1/In2 mixture occupies cages of coordination number (CN) 14 in the form of a tetragonal prism which is capped on all faces. The Tm2 atoms have the higher coordination number 16. The nickel atoms center tri-capped trigonal prisms (CN 9) and the indium atoms occupy base-capped square antiprisms (CN 10).

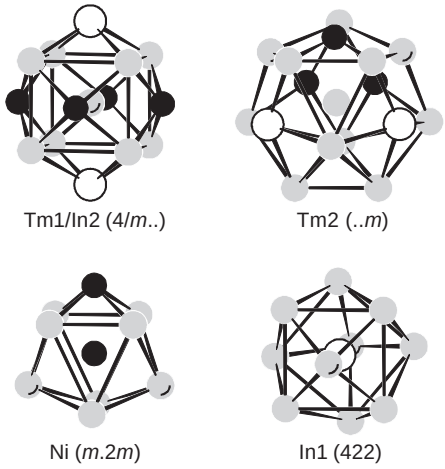

Fig. 4. Coordination polyhedra in the $Tm_{4.83(3)}Ni_2In_{1.17(3)}$ structure. Thulium, nickel, and indium atoms are drawn as grey, black filled, and open circles, respectively. The site symmetries are given in parentheses. Atoms marked with a crescent indicate Tm/In mixing.

Acknowledgments

We are grateful to Dipl.-Ing. U.Ch. Rodewald and B. Heying for the intensity data collections. This work was supported by the Deutsche Forschungsgemeinschaft. M.L. is indebted to the NRW Graduate School of Chemistry for a Ph.D. stipend.

References

[1] Ya.M. Kalychak, J. Alloys Compd. 262–263 (1997) 341.
[2] Ya.M. Kalychak, V.I. Zaremba, R. Pöttgen, M. Lukachuk, R.-D. Hoffmann, Rare earth-transition metal-indides, in: K.A. Gschneider Jr., V.K. Pecharsky, J.-C. Bünzli (Eds.), Handbook on the Physics and Chemistry of Rare Earths, Elsevier, Amsterdam, 2005, Chapter 218.
[3] V.I. Zaremba, I.R. Muts, U.Ch. Rodewald, V. Hlukhyy, R. Pöttgen, Z. Anorg. Allg. Chem., in press.
[4] V.I. Zaremba, V. Hlukhyy, R. Pöttgen, Z. Anorg. Allg. Chem., in press.
[5] V.I. Zaremba, V.M. Baranyak, Ya.M. Kalychak, Vestn. Lvov Univ., Ser. Khim. 25 (1984) 18.
[6] V.I. Zaremba, V.K. Bels'kii, Ya.M. Kalychak, V.K. Pecharskyy, E. Gladyshevskyy, Dopov. Akad. Nauk URSR B (1987) 42.
[7] R. Ferro. R. Marazza, G. Rambaldi, Z. Anorg. Allg. Chem. 410 (1974) 219.
[8] Ya.M. Kalychak, V.I. Zaremba, Yu.B. Tyvanchuk, Sixth International Conference on the Crystal Chemistry of Intermetallic Compounds, Lviv, Ukraine, 1995. 77pp.
[9] V.I. Zaremba, Ya.M. Kalychak, P.Yu. Zavalii, V.A. Bruskov, Krystallografiya 36 (1991) 1415.
[10] V.I. Zaremba, V.A. Bruskov, P.Yu. Zavalii, Ya.M. Kalychak, Izv. Akad. Nauk SSSR, Neorg. Mater. 24 (1988) 409.
[11] Ya.M. Kalychak, V.I. Zaremba, V.M. Baranyak, P.Yu. Zavalii, V.A. Bruskov, L.V. Sysa, O.V. Dmytrakh, Neorg. Mater. 26 (1990) 94.
[12] M. Lukachuk, Ya.M. Kalychak, R. Pöttgen, R.-D. Hoffmann, Z. Kristallogr. 20 (Suppl.) (2003) 142.
[13] M. Lukachuk, Ya.M. Kalychak, R. Pöttgen, Z. Naturforsch. 59B (2004) 893.
[14] R. Pöttgen, Th. Gulden, A. Simon, GIT-Laborfachzeitschrift 43 (1999) 133.
[15] K. Yvon, W. Jeitschko, E. Parthé, J. Appl. Crystallogr. 10 (1977) 73.
[16] Ya.V. Galadzhun, R. Pöttgen, Z. Anorg. Allg. Chem. 625 (1999) 481.
[17] G.M. Sheldrick, SHELXL-97, Program for Crystal Structure Refinement, University of Göttingen, Germany, 1997.
[18] G.M. Sheldrick, SHELXS-97, Program for the Solution of Crystal Structures, University of Göttingen, Germany, 1997.
[19] W. Rieger, H. Nowotny, F. Benesovsky, Monatsh. Chem. 95 (1964) 1502.
[20] W.H. Zachariasen, Acta Crystallogr. 2 (1949) 94.
[21] K. Remschnig, T. LeBihan, H. Noël, P. Rogl, J. Solid State Chem. 97 (1992) 391.
[22] M. Lukachuk, R. Pöttgen, Z. Kristallogr. 218 (2003) 767.
[23] H.J. Becher, R. Krogmann, E. Peisker, Z. Anorg. Allg. Chem. 344 (1966) 140.
[24] A.V. Zelinski, A.A. Fedorchuk, Inorg. Mater. 31 (1995) 1355 translated from Neorg. Mater. 31 (1995) 1491.
[25] A.P. Gonçalves, H. Noël, J.C. Waerenborgh, J. Magn. Magn. Mater. 251 (2002) 1.
[26] F. Fourgeot, P. Gravereau, B. Chevalier, L. Fournès, J. Etourneau, J. Alloys Compd. 238 (1996) 102.
[27] B. Chevalier, F. Fourgeot, D. Laffargue, R. Pöttgen, J. Etourneau, J. Alloys Compd. 275–277 (1998) 537.
[28] J.L. Moriarty, J.E. Humphreys, R.O. Gordon, N.C. Baenziger, Acta Crystallogr. 21 (1966) 840.
[29] P.I. Kripyakevich, M.Yu. Teslyuk, D.P. Frankevich, Sov. Phys. Crystallogr. 10 (1965) 344.
[30] R.C. Mansey, G.V. Raynor, I.R. Harris, J. Less-Common Met. 14 (1968) 329.
[31] J. Emsley, The Elements, Oxford University Press, Oxford, 1999.
[32] R. Pöttgen, R. Dronskowski, Z. Anorg. Allg. Chem. 622 (1996) 355.
[33] J. Donohue, The Structures of the Elements, Wiley, New York, 1974.
[34] B. Aronsson, Acta Chem. Scand. 12 (1958) 31.
[35] F. Bertaut, P. Blum, C. Roy. Acad. Sci. Paris 236 (1953) 1055.